



Interfacial thermal conductance in rapid contact solidification process

W. Wang, H.-H. Qiu *

Department of Mechanical Engineering, Hong Kong University of Science and Technology, Clear Water Bay, Kowloon, Hong Kong

Received 27 December 2000; received in revised form 28 September 2001

Abstract

In this study, an interfacial temperature sensor, having a junction thickness of only 1 μm was developed utilizing micro-fabrication technique. As a simulation of rapid contact solidification process, a sudden falling experiment was conducted. The special sensor was employed to measure the rapid temperature changes at the substrate surface. A simple procedure was proposed for determining the interfacial thermal conductance during the rapid contact process of molten metal (Indalloy-158) with copper substrate. The influence of initial state of molten metal on thermal conductance was investigated. The agreement between the calculated thermal histories and measured ones indicated the validity of the present method. © 2002 Elsevier Science Ltd. All rights reserved.

Keywords: Temperature measurement; Thermal conductance; Solidification

1. Introduction

Rapid contact solidification of a molten metal on a cold substrate is often encountered in many manufacturing processes such as metal casting, micro-droplet-soldering and spray deposition. Because of the roughness of the solid surface, the surface tension of the molten metal, and gas entrapment, a thermal contact resistance, which is expressed as the reciprocal of an interfacial heat transfer coefficient, may be felt at the interface. The rate of the heat transfer from the molten metal to the substrate is often limited by the thermal contact resistance. Previous analysis [1,2] confirmed that the interfacial heat transfer coefficient between the casting and the mold was among the most important variables that controlled the melt cooling and solidification. In addition, it is possible to promote the accuracy of numerical solutions for different solidification models [3–8] if information regarding interfacial heat transfer coefficient is known with sufficient accuracy. It

is therefore essential to investigate interfacial thermal conductance during rapid contact solidification process.

As a practical matter, interfacial heat transfer coefficient is quite difficult to be evaluated directly from experiment. Corresponding to the two different metal–mold interface stages: a nonconforming contact and a clearance gap, Ho and Pehlke [9,10] presented two independent means for determining the time varying interfacial heat transfer coefficient. These two methods are: (1) computer solution of the inverse heat conduction problem using thermocouple measurement at selected locations; (2) measurement of the variation of interfacial gap size with the time, and deriving interfacial heat transfer coefficient from heat transfer data across a static gap. A number of investigators [11–17] have studied interfacial heat transfer under various process conditions. In most studies [11–13], the first method based on finite difference or finite element technique was widely used because the second method is suitable only when a clearance gap forms at the interface. Some researchers [15–18] also quantified interfacial heat transfer coefficient by fitting the experimental data with the computational cooling curves.

However, if any matching methods or inverse technique would be employed to determine interfacial heat

*Corresponding author. Tel.: +852-2358-7190; fax: +852-2358-1543.

E-mail address: meqiu@ust.hk (H.-H. Qiu).

Nomenclature		Subscripts	
c_p	specific heat	0	initial state
H	enthalpy	1	sensor 1
h	interfacial heat transfer coefficient	2	sensor 2
k	thermal conductivity	cop	copper substrate
L	latent heat of fusion	ℓ	liquid region
q	heat flux	j	liquid region ($j = \ell$) or solid region ($j = s$)
T	temperature	m	melting point
<i>Greek symbols</i>		s	solid region
ρ	density	sub	substrate region

transfer coefficient from inner temperature measurements, the locations of temperature sensor should be established very close to the melt–substrate interface. Otherwise, the obtained heat transfer coefficient may be less accurate, because the thermal history at the selected location is insensitive to the change in heat transfer coefficient. But in rapid contact solidification process, it is difficult to locate the sensor very close to the melt–substrate interface, because the sensor will affect the solidification process. So the primary objective of the present study is to develop a special method for recording the rapid temperature changes at the substrate surface without disturbance of solidification process. Once the substrate surface temperature is known, a convenient procedure is expected to be proposed for the determination of interfacial thermal conductance.

Previous studies [12–14] indicate that in metal solidification process, the most important part of heat extraction takes place in the first stages of thermal contact, which has profound influence on the microstructure of the solidified metal. In this work, as a simulation of rapid contact solidification process, a sudden falling experiment was conducted. Cooling curves in the early stages of the rapid contact solidification process were obtained. The interfacial heat transfer coefficient, as a function of time, during the rapid contact process of molten metal (Indalloy-158, a low melting temperature eutectic solder) with copper substrate was determined. The influence of the initial state of molten metal including initial temperature and falling height on the interfacial thermal conductance was also investigated.

2. Development of an interfacial temperature sensor

Because of the simplicity and comparatively rapid response, fine-wire thermocouples are usually employed to measure transient temperatures arises in numerous heat transfer investigation. However, in the present application, the substrate surface temperature during the rapid solidification process is of interest, the perfor-

mance of fine-wire thermocouple is unsatisfactory. The major difficulty is in positioning the junction on the surface without disturbing the solidification process. Furthermore, the minimum size of the junction, which affects the rate of response, is usually limited to the wire diameter. In this section, an interfacial temperature sensor is developed to overcome the difficulties using micro-fabrication technique.

2.1. Principle

The measurement of rapidly changing surface temperature of substrate can be accomplished with a new arrangement. As shown in Fig. 1, a thin layer (1 μm) of constantan (Cu60/Ni40) is deposited to the polished copper substrate surface utilizing sputtering technique. The corresponding lead wires are connected with the copper substrate and the thin film separately. A special T-type thermocouple having a junction thickness of only 1 μm is then obtained. The interface between the constantan layer and the underlying surface of the copper substrate is just the plane at which the thermal EMF (Electro-Motive Force) is generated.

2.2. Fabrication

The substrate is made of copper, its thermophysical properties are summarized in Table 1. The diameter of the substrate is 25.4 mm and the length is 12 mm. “L”-type holes (1 mm diameter) are drilled inside the substrate. The Teflon insulated constantan (Cu60/Ni40)

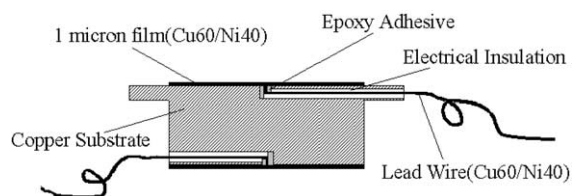


Fig. 1. Cross-section of the substrate combined with the sensor.

Table 1
Thermal properties of copper substrate

	Unit	Copper
ρ	kg/m ³	8940
c_p	J/kg K	$384 + 0.0988T$
k	W/m K	$400 - 0.0614T$

wire (0.2 mm diameter) is inserted into the holes. A small amount of epoxy adhesive (OMEGABOND), which has high thermal conductivity, excellent strength and electrical insulating characteristics, is applied at one end of the wire to hold the wire in place. Then the surface of the copper substrate is polished by a variable speed grinder-polisher (BVEHLER). To make certain there are no metal-to-metal contact between the constantan wire and the copper substrate, a photomicrograph of the polished substrate surface is shown in Fig. 2(a). Notice the absence of any metal contact between the constantan wire and the copper substrate. The final step is to deposit a thin layer (1 μm) of constantan (Cu60/Ni40) to the polished copper substrate surface utilizing sputtering technique. Fig. 2(b) illustrates the photomicrograph of the substrate surface with the deposited thin layer. It shows clearly that the thin layer of constantan has good contact with the copper substrate and the inner constantan wire.

2.3. Calibration

Calibration of the present sensor was performed in a portable block calibrator (OMEGA CL720) capable of multiple set-point temperatures up to 300 °C. With the reference junction being maintained at 0 °C, the voltage at each set point was recorded by a 34401 A Multimeter (Hewlett Packard). The calibration curve obtained is shown in Fig. 3. The calibration data is compared with the EMF response of the standard T-type thermocouple, the great agreement between these results indicates that the present sensor could be considered as a special type-T thermocouple having a junction thickness of only 1 μm .

It is of course desirable to calibrate the sensor under transient conditions, however, because the present special sensor is bounded with the experimental specimen together, a separately fabricated micro sensor and special equipment need to be constructed for this purpose, which should be done in the near future.

2.4. Characteristics

One of the principal factors, which control the response speed of thermocouples, is the time required to heat the junction between two metals. In the present application, the junction between the two metals (copper and constantan) is at the interface between the constantan film and the underlying copper substrate. Heat supplied to the exposed surface of this sensor is required to penetrate only 1 μm of constantan (film thickness) in order to heat the junction. Consequently, very little time is required for this sensor to respond to temperature changes at the exposed surface. It is common practice to characterize the response of a temperature sensor to a no-isothermal change of state of its environment by a thermal time constant. The definition for time constant is different for various environmental changes such as a ramp change, a step change and periodic change [19]. Benedict [19] reported two experimental methods for the determination of time constant. The usual method is based on the step change definition of time constant: to plunge the sensor from an initially different temperature into a constant-temperature bath. Another method is based the ramp change definition of the time constant: the sensor, initially at some uniform temperature, is inserted into an environment whose rate of change of temperature with time is fixed and known. In the present study, the sensor is combined with the experimental specimen together, which is difficulty to adopt either of the above methods to determine time constant. Based on the previous investigation [20,21], the response time for the present sensor is estimated to be in the order of microseconds.

To demonstrate the rapid response of the newly developed temperature sensor a simple experiment shown

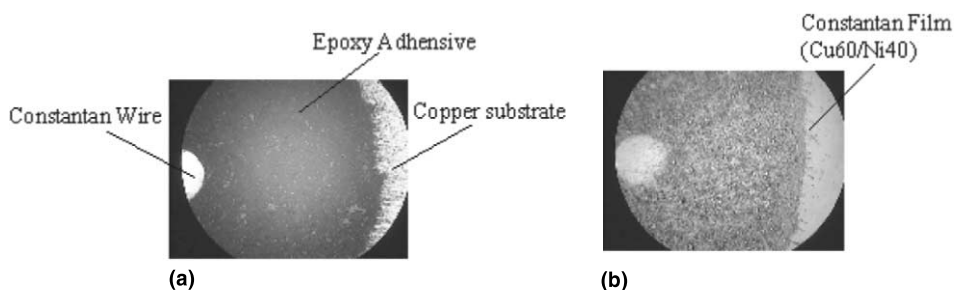


Fig. 2. Photomicrograph of the sensitive surface: (a) polished surface; (b) surface after sputtering.

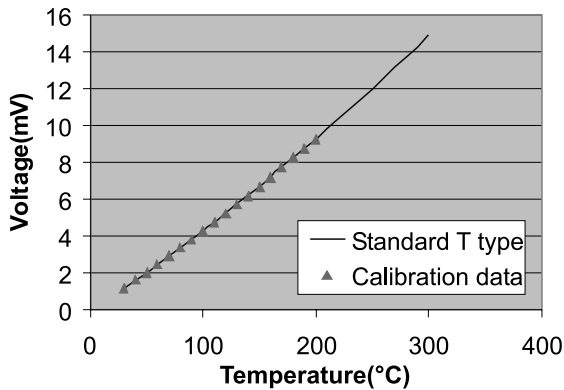


Fig. 3. Calibration curve.

in Fig. 4 was established. A YAG laser (New Wave Gemini 200) that delivers pulses of 200 mJ with 5 ns duration was used to heat the sensor. The sensor's temperature response was recorded with a National Instruments data acquisition board (PCI-6034E, sampling rate: 200 KS/S). Fig. 5 shows the rapid changes in temperature. The maximum temperature change ($62\text{ }^{\circ}\text{C}$) being attained in $5\text{ }\mu\text{s}$ indicates the rapid response of the new sensor, which is much faster than any other commercial available thermocouple.

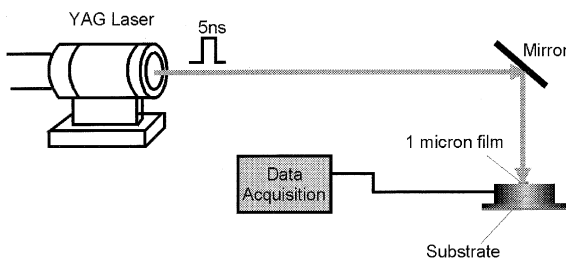


Fig. 4. Schematic diagram of the transient laser heating experiment.

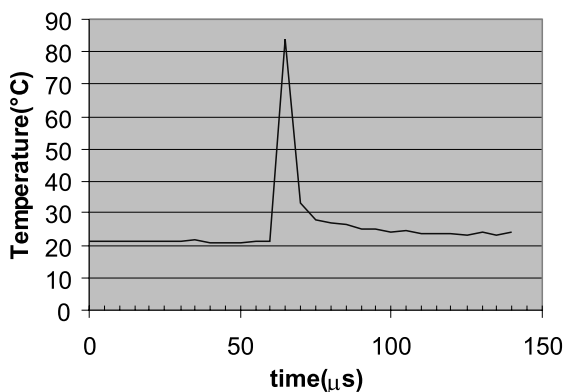


Fig. 5. Rapid temperature response of the newly developed sensor.

Previous study [20] has demonstrated how closely the recorded temperature variation at $1\text{ }\mu\text{m}$ from the exposed surface represents the surface temperature variation. In addition, as the sensor is combined with experimental specimen, disturbance of the solidification process can be avoided. All these characters indicate that the present method can be properly employed to measure the rapid surface temperature changes in the experiment of next section.

The design for the present sensor is specifically suited to the one-dimensional problem mentioned in this study. A modified pattern for the sensor based on the same principle is now under developing for its possible application in multidimensional case. Although the new method presented here is particularly suited to limited metal substrate materials since adhesion between thin film and the substrate is crucial for the success of the temperature measurement, its unusual features may make it worthy of consideration for other applications.

3. Experiment

As a simulation of rapid contact solidification process, a sudden falling experiment is conducted. The main design criterion is to maintain one-dimensional solidification without melt flow effect. The special sensor developed in the above section is employed for the measurement of the top and bottom surface temperatures of the substrate. The cooling curves, in the early stages of the rapid contact solidification process, are obtained.

3.1. Apparatus and instrumentation

As illustrated in Fig. 6, the experimental set up is constituted of three main parts: a cylindrical stainless steel container (25 mm long and 23.6 mm inner diameter); a copper substrate; a linear movement system. The container is used to hold the PCM (phase change material). An electric band heater (25.4 mm length, 25.4 mm inner diameter, 100 W 220 V) is bound up with the container for melting the PCM. A PID temperature controller (Omega CN3003) is used to maintain a stable initial temperature inside the test cell. In order to prevent radial heat losses and the heat flow from the bottom, the cylindrical container is wrapped by a Morgan[®] kaowool ceramic-fiber blanket for insulation, as well as Teflon supporting at the bottom of the container. Two type-K (Omega) thermocouples with small diameter (0.127 mm), sheathed in a 0.159 mm O.D. stainless steel protection tube (Omega), are inserted through the two small holes drilled separately on the container wall. One is located in the central region at a position 5.00 mm from the top surface of the PCM (point 3 in Fig. 6); the other is positioned at 2 mm above the bottom of the

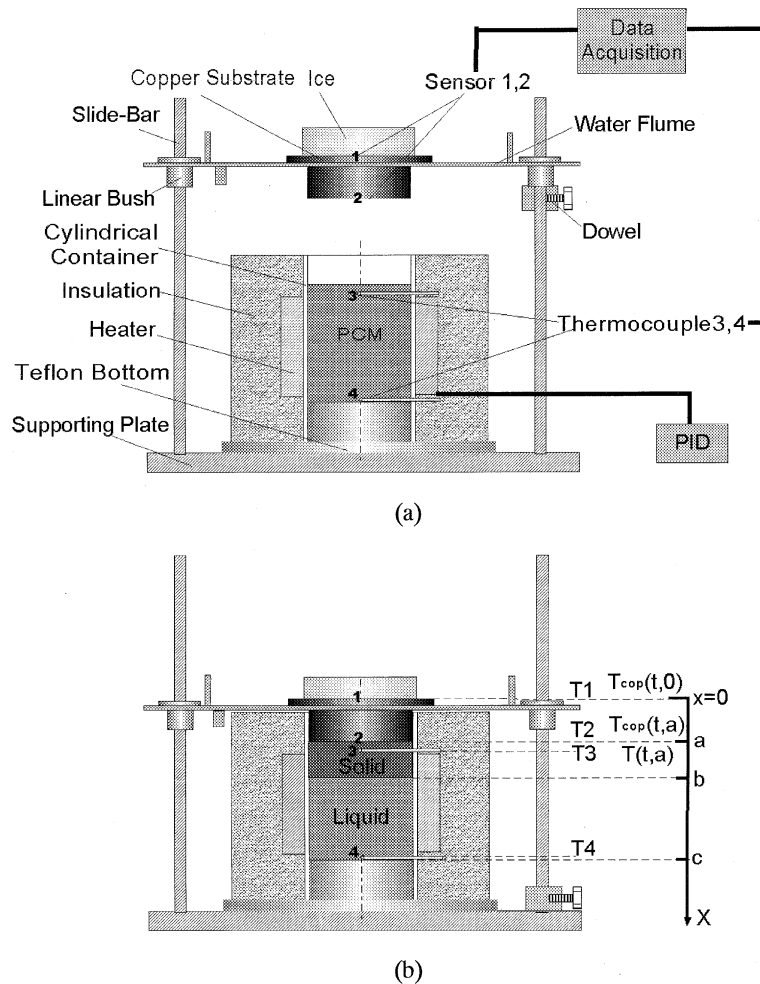


Fig. 6. Rapid contact solidification experiment: (a) initial stage; (b) final stage.

PCM (point 4 in Fig. 6), which is used to monitor the initial uniform temperature of the PCM. The substrate is combined with special sensors 1, 2, which are employed for the measurement of the top and bottom surface temperatures of the substrate. Temperature data from all thermocouples were acquired with a National Instruments data acquisition board (AT-MIO-16). The linear movement system is designed to put the substrate into sudden contact with the molten metal, which can simulate the rapid contact solidification process without the melt flow effect.

Because of the ease of handling and the reasonable cost, Indalloy-158, a low melting temperature eutectic solder, is selected to be the working material (PCM) in this experiment. The melting point of Indalloy-158 is 70 °C and the composition is 49.5 Bi, 27.3 Pb, 13.1 Sn, and 10.1 Cd. The published fluids properties of Indalloy-158 are not available, so the thermal properties given for Lipowiz eutectic with the similar composi-

tion (50 Bi, 26.7 Pb, 13.3 Sn, 10 Cd) summarized by Gau and Viskanta [22] are used, which are listed in Table 2.

The PCM region was initially kept at a uniform temperature 75 °C which was a little higher than the melting point of the metal. The initial temperature of the substrate was kept around 0 °C utilizing ice, which was much lower than the melting point of the metal. For time $t > 0$, the substrate fell suddenly down on to the

Table 2
Thermal properties of Lipowiz eutectic

	Unit	Solid	Liquid
ρ	kg/m ³	9400	9400
c_p	kJ/kg K	0.167	0.167
k	W/m K	19.0	5.499
L	kJ/kg	32.6	
T_m	°C	70.0	

PCM surface from the falling height of 2.0×10^{-2} m. The solidification took place as a result of rapid contacting of the substrate with the PCM.

Under the same boundary condition and initial condition for the substrate, repeat the experiment by changing the initial temperature of the PCM to be 86 °C.

Changed the falling height to be 4.0×10^{-2} m, repeat the same experiment with the initial temperature of the PCM is 75 °C.

3.2. Experimental results

Fig. 7 describes the measured cooling curves in the early stage of the rapid contact process with different superheat or different falling height. The sensors 1, 2 recordings correspond to the measurement in the substrate region. Sensor 3 matches the measurement done in the PCM region. The temperature at point 3 inside the PCM decreased slowly with time, while in the substrate region, the substrate surface temperature measured by sensor 2 quickly reached a peak value, once the liquid–solid contact had been established. The temperature then decreased closely to room temperature. The com-

parison between Figs. 7(a) and (b) indicate that the higher the superheat, the higher the peak values. While comparison between Figs. 7(a) and (c) illustrate that the larger the fall height, the higher the peak values.

4. Determination of interfacial thermal conductance

As described in the above section, the PCM and the substrate were separately kept at different uniform temperature T_0 and T_{cop0} when time $t = 0$. For time $t > 0$ the solidification takes place as a result of rapid contact of the substrate with the PCM, the solid–liquid interface moves in positive x direction as shown in Fig. 6(b). This heat transfer process can be approximated by one-dimensional conduction both in PCM and substrate.

Interfacial heat transfer coefficient $h(t)$ is calculated from its definition equation as follows:

$$h(t) = \frac{q(t, a)}{T(t, a) - T_{cop}(t, a)}, \tag{1}$$

where $q(t, a)$ is heat flux at interface, $T_{cop}(t, a)$ is the substrate surface temperature and $T(t, a)$ is the PCM

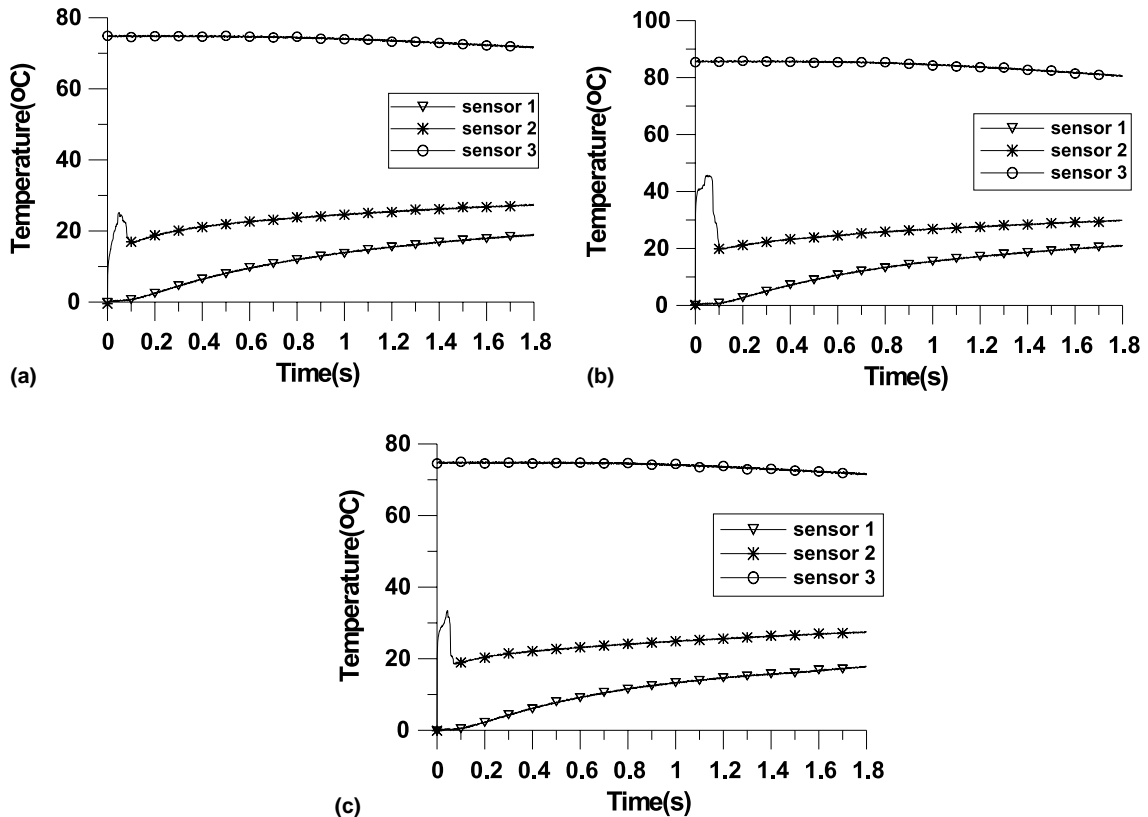


Fig. 7. Measured cooling curves: (a) $T_0 = 75$ °C, falling height = 2 cm; (b) $T_0 = 86$ °C, falling height = 2 cm; (c) $T_0 = 75$ °C, falling height = 4 cm.

surface temperature at $x = a$. $T_{\text{cop}}(t, a)$ is measured by the special sensor. $q(t, a)$ is determined by solving the heat conduction problem in substrate region. $T(t, a)$ is obtained by solving heat conduction problem with phase change in the PCM region. Interfacial heat transfer coefficient can be finally computed from Eq. (1).

4.1. Determination of heat flux

The energy equation for the substrate region is

$$\rho_{\text{cop}} c_{\text{pcop}} \frac{\partial T_{\text{cop}}}{\partial t} = k_{\text{cop}} \frac{\partial^2 T_{\text{cop}}}{\partial x^2} \quad \text{in } 0 < x < a, t > 0, \quad (2)$$

$$T_{\text{cop}}(t, 0) = T_1(t) \quad \text{at } x = 0, t > 0, \quad (3)$$

$$T_{\text{cop}}(t, a) = T_2(t) \quad \text{at } x = a, t > 0, \quad (4)$$

$$T_{\text{cop}}(0, x) = T_{\text{cop}0} \quad \text{at } t = 0, \text{ in } 0 \leq x \leq a. \quad (5)$$

The boundary conditions $T_1(t)$ and $T_2(t)$ are the temperature histories recorded by the special sensors 1, 2, as presented in Fig. 7. By solving this heat conduction problem numerically, the heat flux $q(t, a)$ is obtained, which will be used as one boundary condition for PCM region. The time evolutions of the heat flux at the interface for different superheat and falling height are presented in Fig. 8.

4.2. Determination of interfacial heat transfer coefficient

The mathematical formulation for the PCM region is

$$\rho_j c_{pj} \frac{\partial T_j}{\partial t} = \frac{\partial}{\partial x} \left(k_j \frac{\partial T_j}{\partial x} \right) \quad j = \ell \text{ or } s \quad (6)$$

$$\text{in } a < x < c, t > 0,$$

$$k_j \frac{\partial T_j}{\partial x} = q(t, a) \quad \text{at } x = a, t > 0, \quad (7)$$

$$\frac{\partial T_j}{\partial x} = 0 \quad \text{at } x = c, t > 0, \quad (8)$$

$$T_j = T_0 \quad \text{at } t = 0 \text{ in } 0 \leq x \leq c. \quad (9)$$

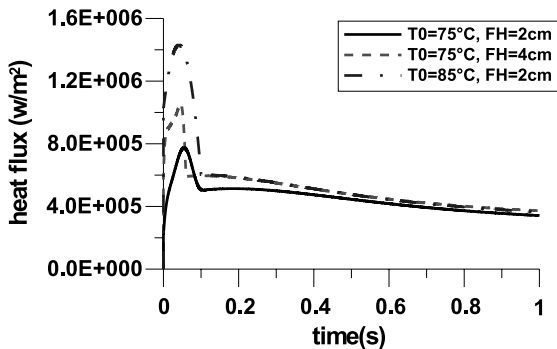


Fig. 8. Evolution of heat flux (FH: falling height).

To alleviate the tracking of the moving interface, the enthalpy method with implicit finite-difference scheme is employed to solve the aforementioned phase change problem, which has been successfully used to handle the rapid phase change problems [8,13,23]. Applying the enthalpy transformation:

$$H = \int_{T_0}^T c_p dT. \quad (10)$$

The energy equation for the PCM region (Eq. (6)) can be rewritten in the enthalpy form

$$\rho_j \frac{\partial H_j}{\partial t} = k_j \frac{\partial^2 T_j}{\partial x^2} \quad \text{in } 0 < x < c, t > 0, \quad (11)$$

where the temperature is related to the enthalpy by the following relations:

$$T_j = \begin{cases} \frac{H_j}{c_p} & H_j < c_p T_m, \\ T_m & c_p T_m \leq H_j \leq (c_p T_m + L), \\ \frac{H_j - L}{c_p} & H_j > (c_p T_m + L). \end{cases} \quad (12)$$

The temperature distribution including the surface temperature $T(t, a)$ in the PCM region is obtained by solving the heat conduction problem with phase change.

Once $q(t, a)$, $T(t, a)$ and $T_{\text{cop}}(t, a)$ is known. The change in interfacial heat transfer coefficient with time for different superheat and falling height is then calculated and presented in Fig. 9.

The above procedure for the determination of the interfacial heat transfer coefficient is so simple because no inverse method or matching technique is used.

5. Discussion

5.1. Variation in interfacial thermal conductance

As noticed from Fig. 9, interfacial heat transfer coefficient rises rapidly from initial contact to a

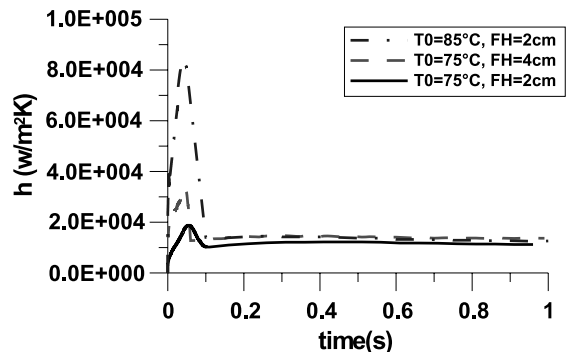


Fig. 9. Evolution of interfacial heat transfer coefficient (FH: falling height).

maximum value and drops closely to an almost constant value thereafter. The rise in heat transfer coefficient from an initial low value to a peak value is well established under various processes [12,14,16], but the time to attain the peak value varies from less than 1 s to more than 30 s [12]. The result illustrated in Fig. 9 demonstrates that this time interval is less than 0.1 s in the rapid contact solidification process. Within the initial period, the dominant factors controlling thermal contact resistance include the wetting ability of the substrate surface by the molten metal. Once the thermal contact has been established with the molten metal, increased wetting ability of the substrate surface tends to maintain a better thermal contact between the melt and the substrate, which produces the initial increase in thermal conductance. With the onset of solidification, the interface contact begins to change from a liquid–solid contact to a solid–solid contact, which leads to the decrease in thermal conductance.

Finally, the interface contact is reduced to a stabilized solid–solid contact when the solidified crust becomes thick enough, which makes the almost constant value of interfacial heat transfer coefficient being maintained.

5.2. Effect of superheat, falling height

Fig. 9 also indicates that in general, the interfacial heat transfer coefficient increase with elevated melt superheat, which is agree with the previous studies [12,16]. A combination of increased fluidity of the molten metal and a larger initial driving force for heat extraction with increasing superheat can explain this increase in thermal conductance. Muojekwu et al. [12] demonstrated that the surface of the solidified shell became smoother as the superheat increased, which implied that the influence of superheat on heat extraction could be attributed to an increase in the interfacial contact.

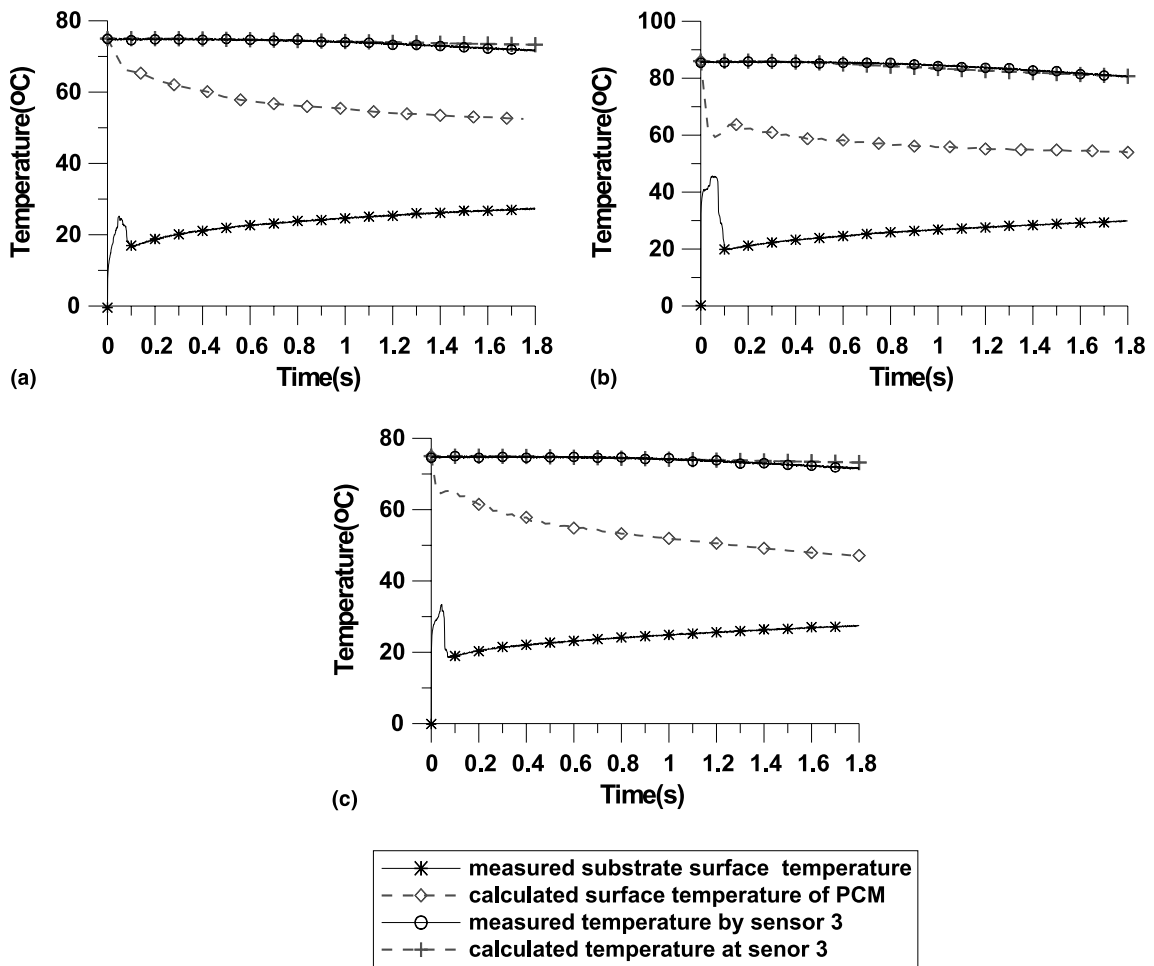


Fig. 10. Temperature evolution: (a) $T_0 = 75\text{ }^\circ\text{C}$, falling height = 2 cm; (b) $T_0 = 86\text{ }^\circ\text{C}$, falling height = 2 cm; (c) $T_0 = 75\text{ }^\circ\text{C}$, falling height = 4 cm.

The effect of falling height on interfacial thermal conductance is also illustrated in Fig. 9. The interfacial heat transfer coefficient increases with increasing falling height. This is because that the contact pressure increases with the elevated falling height, which produces a better interfacial contact at the beginning.

5.3. Validation of the present method

As indicated above, the results obtained in this work showed reasonable tendency when compared with the previous study. To demonstrate the accuracy of the results, the calculated thermal histories are also compared with the measured temperatures at the same location (point 3) in the PCM region. Comparison results as well as the temperature evolution at the substrate/PCM interface are all presented in the Fig. 10. Good agreement between the calculation and computation results is observed from Fig. 10, which demonstrates the validity of the present method.

5.4. Effect of thin film

In most cases, thermal contact between the molten metal and the copper surface is of interest. However, in

the present study, since a thin film of constantan is coated on the copper substrate surface, the interfacial thermal conductance obtained above is actually for the thermal contact between the molten metal and the constantan film. In order to obtain an accurate value for thermal contact between molten metal and the copper surface, it is of course desirable to deposit a thin layer of copper on a constantan substrate. In this study, a copper substrate with a thin film of constantan was used because of the high cost of constantan. In reality, the surface properties such as surface roughness and wetting ability are very important in the process of interfacial heat transfer. The surface roughness of the polished copper surface before and after the sputtering process were measured using WYKO NT3300 profiling system (VEECO). Fig. 11 documents the 3-D interactive display for the two surfaces. The average surface roughness of the copper surface before sputtering is 57.6 nm, and it is 54.3 nm after sputtering, which shows a difference only about 5%. The concept of the critical surface tension has been proposed as a measure of the wettability of solid [24]. An empirical equation has been proposed in literature [24] for describing the relation between contact angle, critical surface tension of the solid and surface tension of the liquid. If surface

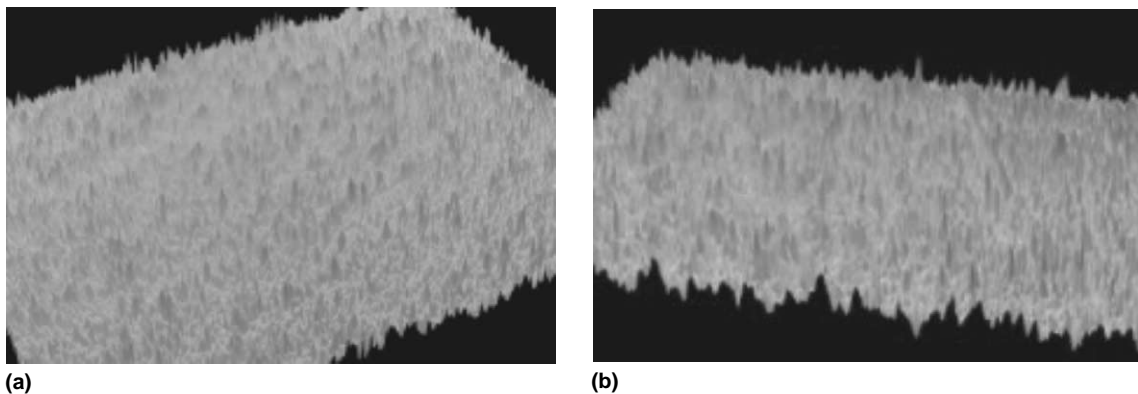


Fig. 11. 3-D interactive display for the surface after sputtering: (a) polished surface before sputtering; (b) surface after sputtering.

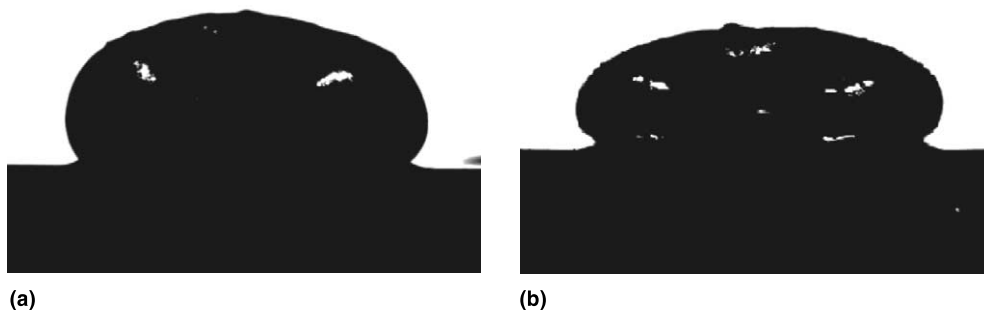


Fig. 12. Drop of molten metal on different surface: (a) copper surface; (b) surface with a constantan film.

tension of the liquid is known as a constant, wettability is determined by contact angle only. The contact angles for a metal droplet (Indalloy-158) on the copper surface and the surface with a thin film of constantan were measured by KRUSS Contact Angle Measuring System G10. The measured contact angles are 140.7° and 141.5° on copper and constantan-film surfaces, respectively. The contact images for the test cases are illustrated in Fig. 12. As the difference in surface roughness and wetting ability between copper surface and surface with a constantan film is very small, we may expect that effect of the constantan thin film on the present interfacial thermal conductance could be ignored. However, this conclusion should be further investigated in the author's future work when a different sensor (constantan substrate with a thin film of copper) is fabricated.

6. Conclusion

In the present study, an interfacial temperature sensor, which has a junction thickness of only $1\ \mu\text{m}$ is developed utilizing micro-fabrication technique. This special sensor can be employed to measure extremely rapid temperature changes at the substrate surface without disturbing the solidification process. The calibration results confirmed the reliability of the present method. The present design of the sensor is specifically suited to one-dimensional case. However, a modified pattern based on the same principle is now under developing for its possible application in multidimensional case. Although the new method is particularly suited to limited metal substrate materials since adhesion between thin film and the substrate is crucial for the success of the temperature measurement, its unusual features may make it worthy of consideration for other applications.

As a simulation of rapid contact solidification process, a sudden falling experiment was conducted. The special sensor was used to record temperature histories at the substrate surface. Once the temperature histories at the substrate surface had been known, a much more simple numerical procedure was proposed for determining thermal conductance during the rapid contact solidification process. In this study, traditional inverse method for estimating thermal conductance from the transient temperature measurement is no longer necessary.

The interfacial heat transfer coefficient, as a function of time, during the rapid contact process of molten metal (Indalloy-158) with copper substrate was determined. The influence of initial stage of the molten metal including melt superheat and falling height on the interfacial thermal conductance was also investigated. The results showed reasonable tendency when compared with the previous study. Furthermore, the accuracy of

the estimated thermal conductance was demonstrated by comparing the calculated thermal histories with the measured temperatures at the same location. The great agreement between these results indicated the validity of the present method.

Acknowledgements

This research was supported by the Hong Kong Government under RGC (Research Grants Council/ Earmarked Grant for Research) Grant Nos. HKUST 6108/97E and HKUST 6043/99E. The authors would like to express their appreciation to Mr. J.Q. Zheng for technical support and Dr. J.D. Tian for his kind assistance in adjusting lasers system.

References

- [1] R.C. Ruhl, Cooling rates in splat cooling, *Mater. Sci. Eng.* 1 (1967) 313–320.
- [2] G.-X. Wang, E.F. Matthys, Modelling of heat transfer and solidification during splat cooling: effect of splat thickness and splat substrate thermal contact, *Int. J. Rapid Solidification* 6 (1991) 141–174.
- [3] G.X. Wang, E.F. Matthys, Numerical modelling of phase change and heat transfer during rapid solidification process: use of control volume integrals with element subdivision, *Int. J. Heat Mass Transfer* 35 (1992) 141–151.
- [4] G. Trapaga, E.F. Matthys, J.J. Valencia, J. Szekely, Fluid flow, heat transfer and solidification of molten metal droplets impinging on substrate: comparison of numerical and experimental results, *Metall. Trans. B* 23 (1992) 701–718.
- [5] T. Bennett, D. Poulikakos, Heat transfer aspects of splat-quench solidification: modeling and experiment, *J. Mater. Sci.* 29 (1994) 2025–2039.
- [6] A.Y. Tong, B.R. Holt, A numerical correlation for the solidification of liquid metal droplets impacting onto a substrate, in: *2nd International Symposium on Multiphase Flows and Heat Transfer on Material Processing*, Atlanta, 1996.
- [7] R.H. Rangel, X. Bian, Undercooling and contact resistance in stagnation – flow solidification on a semi-infinite substrate, *Int. J. Heat Mass Transfer* 41 (1998) 1645–1653.
- [8] M. Pasandideh-Fard, R. Bhola, S. Chandra, J. Mostaghimi, Deposition of tin droplets on a steel plate: simulations and experiments, *Int. J. Heat Mass Transfer* 41 (1998) 2929–2945.
- [9] K. Ho, R.D. Pehlke, Transient methods for determination of metal–mold interfacial heat transfer, *AFS Trans.* 91 (1983) 689–698.
- [10] K. Ho, R.D. Pehlke, Mechanisms of heat transfer at a metal–mold interface, *AFS Trans.* 92 (1984) 587–598.
- [11] K. Ho, R.D. Pehlke, Metal–mold interfacial heat transfer, *Metall. Trans. B* 16 (1985) 585–596.
- [12] C.A. Muojekwu, I.V. Samarasekera, J.K. Brimacombe, Heat transfer and microstructure during the early stages of

- metal solidification, *Metall. Mater. Trans. B* 26 (1995) 361–382.
- [13] T. Loulou, E.A. Artyukhin, J.P. Bardon, Estimation of thermal contact resistance during the first stages of metal solidification process: I – Experiment principle, *Int. J. Heat Mass Transfer* 42 (1999) 2119–2127.
- [14] T. Loulou, E.A. Artyukhin, J.P. Bardon, Estimation of thermal contact resistance during the first stages of metal solidification process: II – Experimental setup and results, *Int. J. Heat Mass Transfer* 42 (1999) 2129–2142.
- [15] N.A. El-Mahallawy, A.M. Assar, Metal–mold heat transfer coefficient using end-chill experiments, *J. Mater. Sci. Lett.* 7 (1988) 205–208.
- [16] N.A. El-Mahallawy, A.M. Assar, Effect of melt superheat on heat transfer coefficient for the aluminium solidifying against copper chill, *J. Mater. Sci.* 26 (1991) 1729–1733.
- [17] G.X. Wang, E.F. Metthys, Experimental investigation of interfacial thermal conductance for molten metal solidification on a substrate, *J. Heat Transfer* 118 (1996) 157–163.
- [18] W.D. Griffiths, The heat-transfer coefficient during the unidirectional solidification of an Al–Si alloy casting, *Metall. Mater. Trans. B* 30 (1999) 473–482.
- [19] R.P. Benedict, in: *Fundamentals of Temperature, Pressure, and Flow Measurements*, third ed., Wiley, New York, 1984, pp. 253–263.
- [20] D. Bendersky, A special thermocouple for measuring transient temperatures, *Mech. Eng.* 75 (2) (1953) 117–121.
- [21] J.M. Hagar, S. Simmons, D. Smith, S. Onishi, L.W. Langley, T.E. Diller, Experimental performance of a heat flux microsensor, *J. Eng. Gas Turbines Power* 113 (1991) 246–250.
- [22] C. Gau, R. Viskanta, Melting and solidification of a metal system in a rectangular cavity, *Int. J. Heat Transfer* 27 (1) (1984) 113–123.
- [23] A.Y. Tong, B.R. Holt, Numerical study on the solidification of liquid metal droplets impacting onto a substrate, *Numer. Heat Transfer A* 31 (1997) 797–817.
- [24] A. Frohn, N. Roth, in: *Dynamics of Droplets*, Springer, Berlin, 2000, pp. 8–9.